J. Chem. Sci. Vol. 128, No. 7, July 2016, pp. 1047–1055. © Indian Academy of Sciences.
DOI 10.1007/s12039-016-1112-2

Crystal structures of unsymmetrically mixed β-pyrrole substituted nickel(II)-*meso*-tetraphenylporphyrins

BHYRAPPA PUTTAIAH*, VELKANNAN VEERAPANDIAN and SARANGI UJWAL KUMAR
Department of Chemistry, Indian Institute of Technology Madras, Chennai, Tamil Nadu State 600 036, India
e-mail: byra@iitm.ac.in

MS received 8 April 2016; revised 15 May 2016; accepted 18 May 2016

Abstract. Crystal structures of solvated unsymmetrically substituted *meso*-tetraphenylporphyrins, 2,3,12,13,17-pentachloro-5,7,8,10,15,18,20-hepta-phenylporphyrin, $H_2TPP(Ph)_3(Cl)_5$, **1** and its nickel(II), $NiTPP(Ph)_3(Cl)_5$, **2** were determined by single crystal XRD analysis. In addition, a new unsymmetrically substituted porphyrin, 2,3,12,13,17-pentacyano-5,7,8,10,15,18,20-heptaphenyl-porphinato nickel(II) complex, $NiTPP(Ph)_3(CN)_5$, **3** complex was synthesized and its solvated structure was examined by crystallography. These porphyrins exhibited dramatic nonplanar conformation of the macrocycle as evidenced from the average displacement of the β-pyrrole carbon ($\pm\Delta C_\beta$) from the mean plane of the porphyrin ring and the trend in nonplanarity varies in the order: **2** (1.189(5) Å) > **1** (1.036(6) Å) > **3** (0.895(6) Å). The normal-coordinate structural decomposition analysis of these structures revealed mainly *saddle* distortion of the macrocycle combined with small degree of *ruffled* or *domed* distortions. The Hirshfeld surface analysis of structures **1-3** revealed solvate dependent intermolecular contacts with varying degree of H. . .H (43–49%), C. . .H (17–19%), H. . .Cl (25–30%) and N. . .H (∼19%) contact contributions.

Keywords. Unsymmetrical mixed substituted porphyrins; β-pyrrole substituted porphyrins; NSD analysis; Hirshfeld surface analysis.

1. Introduction

Synthetic porphyrin analogues are of considerable interest owing to their use as model compounds.[1–3] Besides, substituted porphyrin systems have also been widely used in potential material applications such as molecular sieves,[4,5] catalysis,[6–12] sensors,[13–19] nonlinear optics,[20,21] and dye sensitized solar cells.[22–24] The core metal ion, peripheral substituents and nonplanarity of the macrocycle alter the electronic properties of the porphyrin π-system.[25,26] The peripheral substituents produce unique physicochemical properties including varied degree of distortion of the tetrapyrrole.[27] Moreover, the nonplanarity of the sterically crowded porphyrins is induced by the repulsive interactions among the peripheral substituents.[28,29] Normal-coordinate structural decomposition (NSD) analysis of the heme in various heme proteins feature interesting trend in distortion of the macrocycle.[30]

Numerous crystal structure reports are available on variety of substituted porphyrins and metalloporphyrins.[31–38] Systematic analyses of the change in conformation of the macrocycle as a function of core metal ion and the substituents have been well documented in the literature.[27] Metallotetraphenylporphyrins, MTPPs are known to form porphyrin sponges with varying degree of lattice solvates.[39,40] The introduction of mixed substituents at all the β-pyrrole positions of MTPPs revealed varying degree of nonplanarity of the porphyrin ring.[41–43] The unsymmetrically mixed β-pyrrole substituted porphyrins, $MTPP(Ph)_3(X)_5$ produced unusual trend in physicochemical properties.[43,44] To examine the role of size of the unsymmetrical β-pyrrole substituents on the structural variations of the porphyrin ring, 2,3,12,13,17-pentacyano-5,7,8,10,15,17,20-heptaphenylporphinato nickel(II), $NiTPP(Ph)_3(CN)_5$ was synthesized and characterized by single crystal XRD analysis. Furthermore, the crystal structures of 2,3,12,13,17-pentachloro-5,7,8,10,15,17,20-heptaphenylporphyrin and its Ni(II) complex, $MTPP(Ph)_3(X)_5$ (M=2H and Ni(II); X=Cl) are also reported in this work (Figure 1). The Hirshfeld surface analysis of the structures revealed interesting intermolecular short contacts.

2. Experimental

2.1 *Instrumentation*

Electronic absorption spectra of porphyrins were recorded on a JASCO V550 model spectrophotometer using a pair of quartz cells of 1 cm path length in CH_2Cl_2 at 298K. ^1H NMR spectra of porphyrins were

*For correspondence

recorded on a Bruker Avance 400 MHz spectrometer using $CDCl_3$ solvent with tetramethylsilane as an internal reference at room temperature. Mass spectral measurements of the porphyrins were carried out using electrospray ionization (ESI) mass spectrometer model Micromass Q-TOF Micro using 10% formic acid in methanol as solvent medium. The single crystal XRD data collection was carried out on a Bruker model APEX II CCD diffractometer equipped with liquid nitrogen cryostat. The crystals were coated with paratone oil and mounted on a glass fiber attached to a goniometer.

2.2 *Materials*

Porphyrins, $MTPP(Ph)_3(X)_5$ (M = 2H and Ni(II); X = Cl) were prepared as described previously[43,44] and their observed data is consistent with the reported literature data. The new porphyrin complex, $NiTPP(Ph)_3(CN)_5$ was synthesized and characterized by electronic absorption, ^{1}H NMR and high resolution mass spectroscopic methods. All the solvents employed in this study were of analytical grade and used as received.

2.3 *Crystal structures*

Single crystals of $MTPP(Ph)_3Cl_5$ (M = 2H and Ni(II)) were grown by vapor diffusion of *n*-hexane to the saturated solution of individual porphyrins separately in 1,2-dichloroethane (DCE) over a period of five-to-seven days at 298 K. Similarly, crystals of $NiTPP(Ph)_3(CN)_5$ were grown by diffusion of hexane vapour to the porphyrin in toluene over a period of 10 days at 298 K.

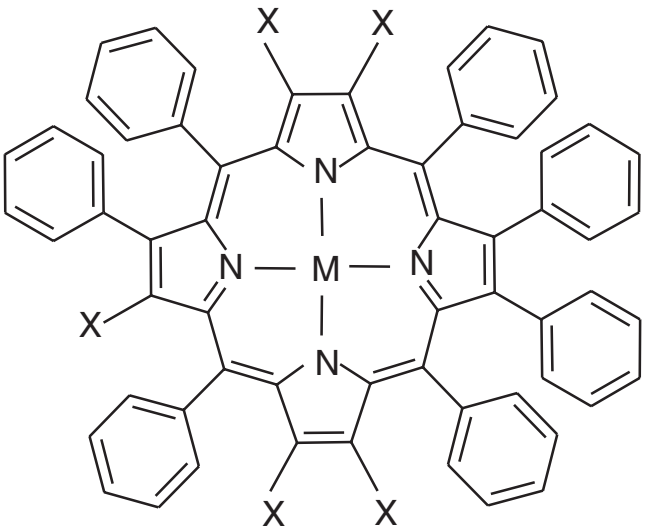

Figure 1. Molecular structure of unsymmetrically mixed substituted porphyrins.

Crystal structures were solved by direct methods using WINGX32[45] SIR92 (WINGX) program[46] was used to solve the structures by direct methods. The non-hydrogen atoms were determined by successive Fourier synthesis by full matrix least-squares refinement on $|F|^2$ using SHELXL97 software. Non-hydrogen atoms were refined with anisotropic thermal parameters. All the hydrogen atoms in the porphyrin structure could not be located and were fixed at chemically meaningful positions and given riding model refinement. ORTEPs were generated using ORTEP-3 program[47] and the intermolecular short contacts were analysed using Mercury version 3.5 software.[48]

Crystallographic information files for the crystal structures with their CCDC numbers of 1037867 for **1**, 1037868 for **2** and 1037869 for **3** can be obtained free of charge from the Cambridge Crystallographic Data Centre via www.ccdc.cam.ac.uk/data_request/cif.

Hirshfeld surface calculations[49] of the porphyrin structures were carried out using their crystallographic information files with crystal explorer 3.1 program.[50] Hirshfeld surface analysis was carried out using a standard (high) surface resolution.[51] For a given structure, Hirshfeld surface is unique for a set of spherical atomic electron densities. The d_{norm} values were mapped onto the Hirshfeld surface by employing blue-red-white color scheme: red regions for close contacts with negative d_{norm} values; blue regions represents longer contacts with positive d_{norm} values; white regions indicates the distance contacts corresponding to the van der Waals separation with $d_{norm} = 0$. The 3-D d_{norm} was resolved into 2-D fingerprint plots by quantitatively summarizing[52,53] the nature and type of all the intermolecular contacts in the crystal lattice.

$NiTPP(Ph)_3(CN)_5$: $NiTPP(Ph)_3Br_5$[43,44] and its cyanation was carried out using modified reported procedure[54] with 7 fold excess of CuCN. $NiTPP(Ph)_3Br_5$ (0.130 g, 0.10 mmol) was dissolved in dry pyridine (30 mL). To this, CuCN (0.45 g, 5.02 mmol) was added in the solid form. Then, the reaction mixture was stirred and refluxed for 48 h under argon atmosphere. At the end of this period, the solvent was rotary evaporated under reduced pressure. Further, the resultant residue was re-dissolved in a minimum amount of $CHCl_3$, and it was loaded onto a silica gel column using $CHCl_3$ as the eluent. The desired product was eluted using 2% EtOAc in $CHCl_3$ and the solvent was removed under

reduced pressure. The resultant residue was dried under vacuum at 373 K for 8 h, the yield of product was found to be 0.031 g (30%). Electronic absorption spectral data in CH_2Cl_2: λ_{max}, nm (log ε): 347 (4.29), 382 (sh), 468 (5.09), 546 (3.80), 592 (sh), 646 (4.31). ^{1}H NMR in $CDCl_3$: δ_H (ppm): 8.02 (d, J = 7.6 Hz, 2H, *meso-o*-phenyl-H), 7.60 (t, J = 8.0 Hz, 1H, *meso-p*-phenyl-H), 7.82 (t, J = 7.2 Hz, 2H, *meso-m*-phenyl-H), 7.58 (t, J = 8.0 Hz, 4H, *meso-p*-phenyl-H), 7.42 (m, 5H, *meso*-phenyl-H), 7.16 (m, 12H, *meso* and β-pyrrole-phenyl-H), 7.03 (t, J = 7.6 Hz, 1H, β-pyrrole-*p*-phenyl-H), 6.92 (t, J = 7.6 Hz, 2H, β-pyrrole-*m* and *p*-phenyl-H), 6.86 (m, 1H, β-pyrrole-*p*-phenyl-H), 6.79 (m, 3H, β-pyrrole-*m* and *p*-phenyl-H), 6.70 (m, 2H, β-pyrrole-*m*-phenyl-H). ^{13}C NMR in $CDCl_3$: δ (ppm), 135.28, 134.95, 134.60, 133.62, 130.89, 130.74, 130.60, 130.16, 128.61, 128.16, 127.86, 127.63, 127.29, 110.22. HR ESI MS calculated for $C_{67}H_{36}N_9Ni$ $[M+H]^+$: 1024.2447 (found: 1024.2424).

3. Results and discussion

The preparation of $NiTPP(Ph)_3(CN)_5$ was achieved by cyanation of $MTPP(Ph)_3Br_5$ using the modified reported procedure.[43,44,54] It was characterised by ^{1}H NMR, electronic absorption spectroscopy and mass spectrometry. The electronic spectrum of the complex shows a Soret, B and three Q bands in CH_2Cl_2 at 298 K. It features red-shift of 10 nm in 'B' but blue shift of 8 nm in longest wavelength band relative to the reported symmetrically substituted $NiTPP(Ph)_4(CN)_4$ complex. ^{1}H NMR spectrum of the complex revealed more number of signals in contrast to $NiTPP(Ph)_4(CN)_4$ complex. The *meso*-phenyl protons are down-field shifted by ~0.3–0.6 ppm but β-pyrrole phenyls do not show any significant change in their chemical shifts relative to those reported for $NiTPP(Ph)_4(CN)_4$ in $CDCl_3$ at 298 K.

Crystal structures of $H_2TPP(Ph)_3Cl_5\cdot(C_2H_4Cl_2)_{0.5}$, **1** and $NiTPP(Ph)_3Cl_5\cdot(C_2H_4Cl_2)_2$, **2** were determined by single crystal XRD analysis to elucidate the role of Ni(II) ion on the stereochemistry of the macrocycle. The $NiTPP(Ph)_3(CN)_5\cdot(C_7H_8)_2$, **3** was employed to examine the role of chloro versus cyano group on the stereochemistry of the porphyrin ring. The crystallographic data of the compounds are listed in Table 1. Compound **1** has a molecule of porphyrin and half the DCE solvate in the asymmetric unit (Z = 4). For compound **2**, the asymmetric unit of the structure shows a molecule of porphyrin and two DCE solvates with Z = 2. The structure of **3** shows a porphyrin and two toluene solvates with Z = 1. One of the toluene solvate in this structure shows two disordered positions.

Table 1. Crystallographic data of the structures $H_2TPP(Ph)_3(Cl)_5\cdot(C_2H_4Cl_2)_{0.5}$, **1**; $NiTPP(Ph)_3(Cl)_5\cdot(C_2H_4Cl_2)_2$, **2** and $NiTPP(Ph)_3(CN)_5\cdot(C_7H_8)_2$, **3**.

Structure	**1**	**2**	**3**
Chemical formula	$C_{63}H_{39}Cl_6N_4$	$C_{66}H_{43}Cl_9N_4Ni$	$C_{81}H_{51}N_9Ni$
Formula weight	1064.68	1269.80	1209.02
Crystal system	P 2_1/c	P -1	P 2_1/c
Space group	monoclinic	triclinic	monoclinic
a (Å)	17.7741(12)	13.5407(14)	16.9306(17)
b (Å)	18.9230(15)	14.8204(15)	16.3769(17)
c (Å)	15.3250(12)	14.9946(15)	23.419(2)
α (°)	90.00	96.747(5)	90.00
β (°)	92.152(3)	102.756(4)	105.420(4)
γ (°)	90.00	100.665(4)	90.00
Volume (Å^3)	5150.8(7)	2844.5(5)	6259.6(11)
Z	4	2	4
$D_{calcd.}$ (g/cm^3)	1.373	1.483	1.283
F 000	2188	1296	2512
Crystal size (mm^3)	0.15 × 0.12 × 0.12	0.42 × 0.28 × 0.22	0.24 × 0.22 × 0.18
θ range (°)	1.15–20.07	1.42–25.0	1.25–25.0
Reflections collected	54560	33113	65610
Independent reflections	4850	7869	6626
GOF on F^2	1.062	1.067	1.131
$R_1[I > 2\sigma(I)]$	0.0810	0.0731	0.0887
$wR_2[I > 2\sigma(I)]$	0.2290	0.1970	0.2193

$^a R_1 = \sum \| F_o| - |F_c\| / \sum |F_o|$; $I_o > 2\sigma(I_o)$. $^b wR_2 = [\sum w(F_o^2 - F_c^2)^2 / \sum w(F_o^2)^2]^{1/2}$.

The ORTEP representations of the porphyrin units of structures **1-3** are shown in Figure 2. The selected mean bond lengths, bond angles and geometrical parameters of the structures are listed in Table 2 to examine the role of unsymmetrical substitution on the structural data. Comparison of the structures of **1**-**3** is made with the reported six-coordinated planar $NiTPP(Ph)_4(CN)_4(Py)_2 \cdot Py$ complex to elucidate the influence of planar *versus*

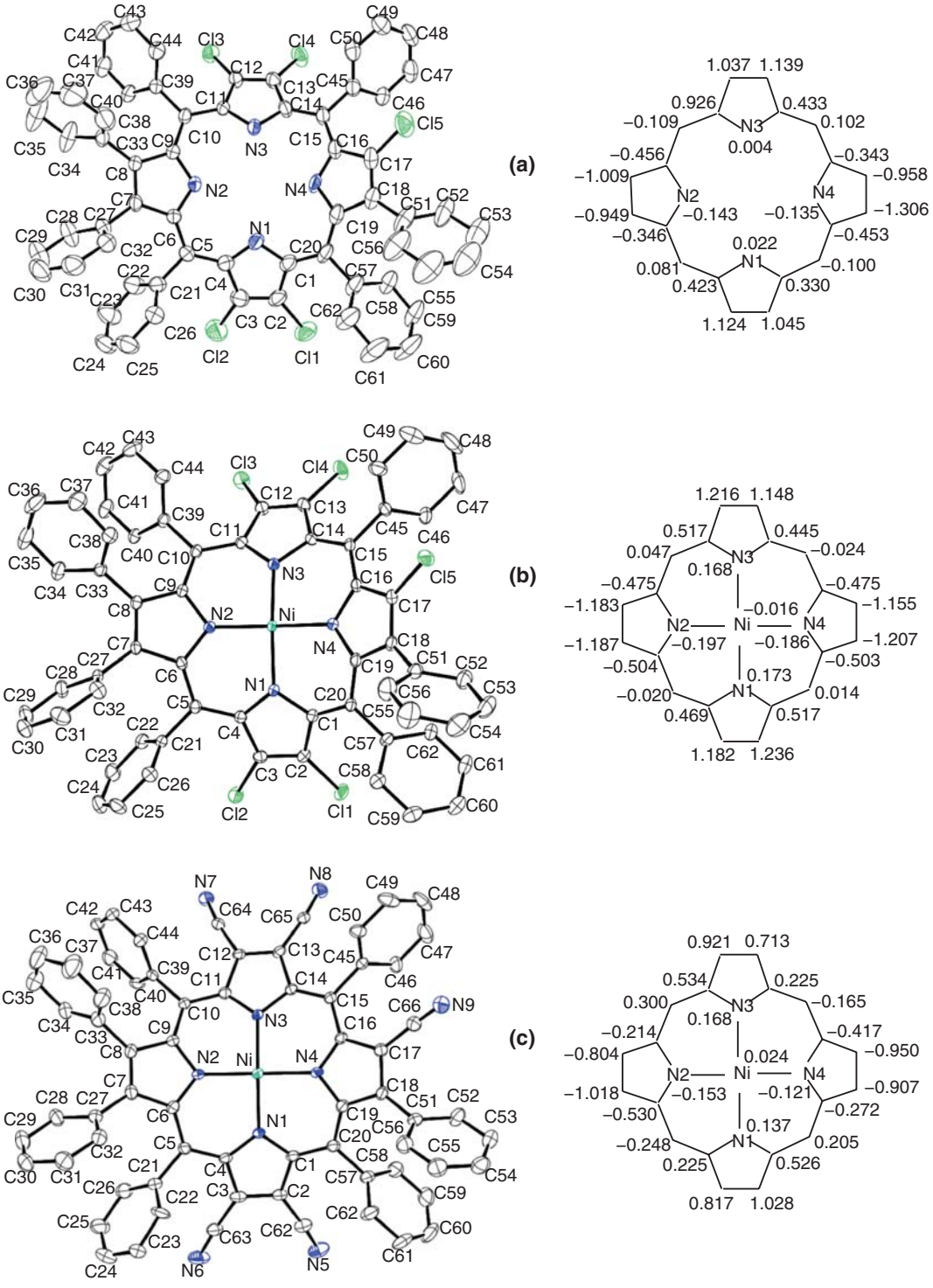

Figure 2. ORTEP drawing **(a)**, **(b)** and **(c)** shown for structures **1**, **2** and **3** respectively. The thermal ellipsoids at 40% probability level 40% for **1**, 30% for both **2** and **3**. The right side shows the displacement of the macrocyclic ring atoms (in Å) from the 24-atom mean plane. The esd's for the displacement values is <0.006 Å.

Table 2. Selected mean bond lengths (Å), bond lengths (°) and geometrical parameters of unsymmetrically substituted porphyrins.

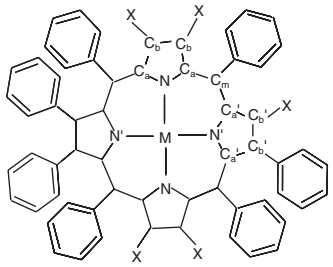

M = 2H, X = Cl, $H_2TPP(Ph)_3Cl_5•(C_2H_4Cl_2)_{0.5}$, **1**
M = Ni(II), X = Cl, $NiTPP(Ph)_3Cl_5•(C_2H_4Cl_2)_2$, **2**
M = Ni(II), X = CN, $NiTPP(Ph)_3(CN)_5•(C_7H_8)_2$, **3**

	1	**2**	**3**	**4**[a]
Ni–N	–	1.907(4)	1.925(4)	2.051(2)
Ni–N′	–	1.905(4)	1.924(4)	2.089(2)
C_b–C_b	1.336(10)	1.350(7)	1.362(9)	1.371(3)
C'_b–C'_b	1.367(11)	1.352(7)	1.356(9)	1.356(3)
C_a–C_m	1.402(10)	1.402(7)	1.389(9)	1.409(3)
C'_a-C_m	1.398(10)	1.389(7)	1.392(9)	1.402(3)
N–C_a–C_m	124.2(7)	122.5(4)	124.6(5)	127.0(2)
N′–C'_a–C_m	123.8(7)	122.5(4)	123.9(6)	125.0(2)
C_a–N–C_a	107.1(7)	106.6(4)	106.6(4)	108.4(2)
C'_a–N′–C'_a	112.3(6)	106.0(4)	105.5(6)	107.3(2)
C_a–C_m–C'_a	123.4(7)	120.1(4)	120.6(6)	125.4(2)
$\Delta C_b(\pm)$, Å	1.071(7)	1.189(5)	0.895(6)	0.0438
Dihedral angle (°) relative to mean plane of the porphyrin ring				
meso-Ph	44.7(2)	42.5(2)	55.4(2)	81.2
β-Ph	55.8(3)	54.3(2)	57.0(2)	80.3
Pyrrole	27.3(3)	29.5(2)	22.1(3)	–

[a]Data of $NiTPP(Ph)_4(CN)_4(Py)_2$ from ref. [54]

nonplanar macrocycle on the typical diagnostic parameters of the 24-atom core.[54] The structures of **1** and **2** showed shorter C_b–C_b bond lengths for the pyrroles with Cl group in contrast to pyrrole with 'Ph' or Ph/Cl groups (C'_b–C'_b) but its Ni(II)-complex, **2** revealed almost similar distances. Structure **1** shows decreased C_b–C_b and C'_b–C'_b bond distances relative to that of the reported structure, $H_2TPP(Ph)_4Cl_4$ (C_b–C_b = 1.345(5) Å and C'_b–C'_b = 1.380(5) Å).[42]

In the case of **1**, N...N separation along the transannular pyrrole direction shows shorter distance (4.010 Å) relative to N′...N′ distance (4.176 Å) along the other transannular pyrrole direction. These distances are shorter than the reported $H_2TPP(Ph)_4(Cl)_4$ structure (N...N = 4.245 Å; N′...N′ = 4.122 Å).[42] The inner NH protons are located exclusively on the opposite pyrroles with phenyls and Ph/Cl bearing pyrroles. As anticipated, the pyrroles with imino hydrogens (NH) shows larger $\angle C'_a$–N′–C'_a than $\angle C_a$–N–C_a (Table 2). This also perhaps indicates the influence of unsymmetrical β-pyrrole substitution on the N_4H_2 core.

The structure of **2** shows comparable Ni–N and Ni–N′ distances but they are shorter than that observed in **3** and this indicates the greater electron-deficient nature of the core nitrogens in the latter than the former structure. The average of Ni–N and Ni–N′ bond lengths in **2** and **3** are longer than those reported for solvated four-coordinated $NiTPP(Ph)_4(CN)_4$[42] (1.892(3) Å)$_{av}$ but comparable to the $NiTPP(CN)_4Br_4$ (1.920 (4) Å)$_{av}$[55] and lower than the six-coordinated Ni(II)-porphyrins.[27] The pyrroles with cyano groups in **3** reveal slightly shorter C_b–C_b bond lengths (1.362(9) Å) than the reported four coordinated $NiTPP(Ph)_4Cl_4$ structure[42] (1.378(6) Å). The less sterically crowded Ni(II)-porphyrins are known to exhibit nonplanar geometry.[27] The enhanced nonplanar distortion in **3** is evidenced from its ΔC_b (± 0.895(6) Å) than the corresponding data of the reported structure, $NiTPP(Ph)_4Cl_4$ (± 0.766(4) Å).[42] Comparison of the diagnostic porphyrin ring parameters, mean $\angle$**N–C_a–C_m** (i.e., average of $\angle$N–C_a–C_m and $\angle$N′–C'_a–C'_m) and mean $\angle C_a$–C_m–C'_a of the macrocycle are decreased in **1-3** in contrast to that of planar structure in **4**. This suggests considerable increase in nonplanarity of the macrocycle in **1-3**. This is also evidenced from the mean displacement of the β-pyrrole carbon, ΔC_b which is dramatically higher

in **1-3** relative to **4**. The structure **1** shows slightly lower ΔC_b ($\pm$1.071(7) Å) than the reported corresponding symmetrically substituted nonplanar structure $H_2TPP(Ph)_4Cl_4$ ($\pm$1.130(4) Å).[42] Further, a comparison of the key porphyrin ring parameters, $\angle$**N–C$_a$–C$_m$** = 124.3(6)°, $\angle C_a$–C_m–C'_a = 120.6(6)° and ΔC_b = $\pm$0.895(6)° Å of solvated $NiTPP(Ph)_3(CN)_5$, **3** (Table 2) are similar to the corresponding data of the reported nonplanar $NiTPP(Ph)_4(CN)_4$ ($\angle$**N–C$_a$–C$_m$**, 123.6(3)° and $\angle C_a$–C_m–C'_a, 119.8(3)° and ΔC_b = $\pm$0.766(4) Å) structure.[42] This suggests that both structures are highly nonplanar with slightly increased distortion in **3** relative to the reported $NiTPP(Ph)_4(CN)_4$ structure.[42]

The significant distortion of the porphyrin ring is also evidenced from the side view of the macrocycle and its linear displacement of the 24 atom core as shown in Figure 3. It can be seen from Figure 3 and Table 2 that the pyrrole groups are tilted up and down from the porphyrin ring mean plane indicating the *saddled* distortion combined with other minor contribution from other distortions. The ΔC_b varies in the order **3** < **1** < **2**. This indicates the decrease in steric crowding in **3** relative to **1** or **2**. The increase in nonplanarity of the macrocycle is also reflected from an increase and decrease in mean dihedral angles for pyrrole and *meso*-phenyl groups, respectively (Table 2).

The extent of intermolecular interactions was examined by molecular packing diagrams. For all the three structures (**1-3**), the molecules are arranged in an offset fashion. In the case of structure **1**, the porphyrins are interacting through C_{Ph}–H...Cl_{Pyr}, C_{Ph}...Cl_{por} and C_{Ph}–H...C_{Ph} short contact distances 2.588–2.941 Å, 3.387 Å and 2.817–2.844 Å, respectively. Structure **2** shows inter-porphyrin [C_{Ph}...C_{Ph} = 3.298 Å, C_{Ph}–H...$C_{Ph/por}$ = 2.84 – 2.88 Å, Cl_{por}...C_{por} = 3.447 Å, 3.410 Å and C_{Ph}–H...Cl_{pyr} = 2.76 – 2.91 Å] and porphyrin...DCE [C_{por}...Cl_{DCE} = 3.397 Å, C_{Ph}...H–C_{DCE} = 2.63–2.80 Å, Cl_{por}...H–C_{DCE} = 2.77 Å, Cl_{DCE}...H–C_{ph} = 2.91 Å and Cl_{por}...Cl_{DCE} = 3.401, 3.453 Å] close contacts. For **3**, intermolecular interactions are dominated mainly *via* inter-porphyrin [C_{ph}–H...C_{Por} = 2.76 – 2.81 Å, C_{ph}–H...C_{por} = 2.74 – 2.79 Å; C_{ph}–H...C_{ph} = 2.79 Å; C_{ph}–H...N_{cyano} = 2.56 – 2.73 Å] and porphyrin...toluene (C_{ph}–H...C_{tol} = 2.79 – 2.86 Å and C_{tol}–H...N_{cyano} = 2.68 Å) close contacts. These short contact distances in structures (**1-3**) suggest the existence of weak

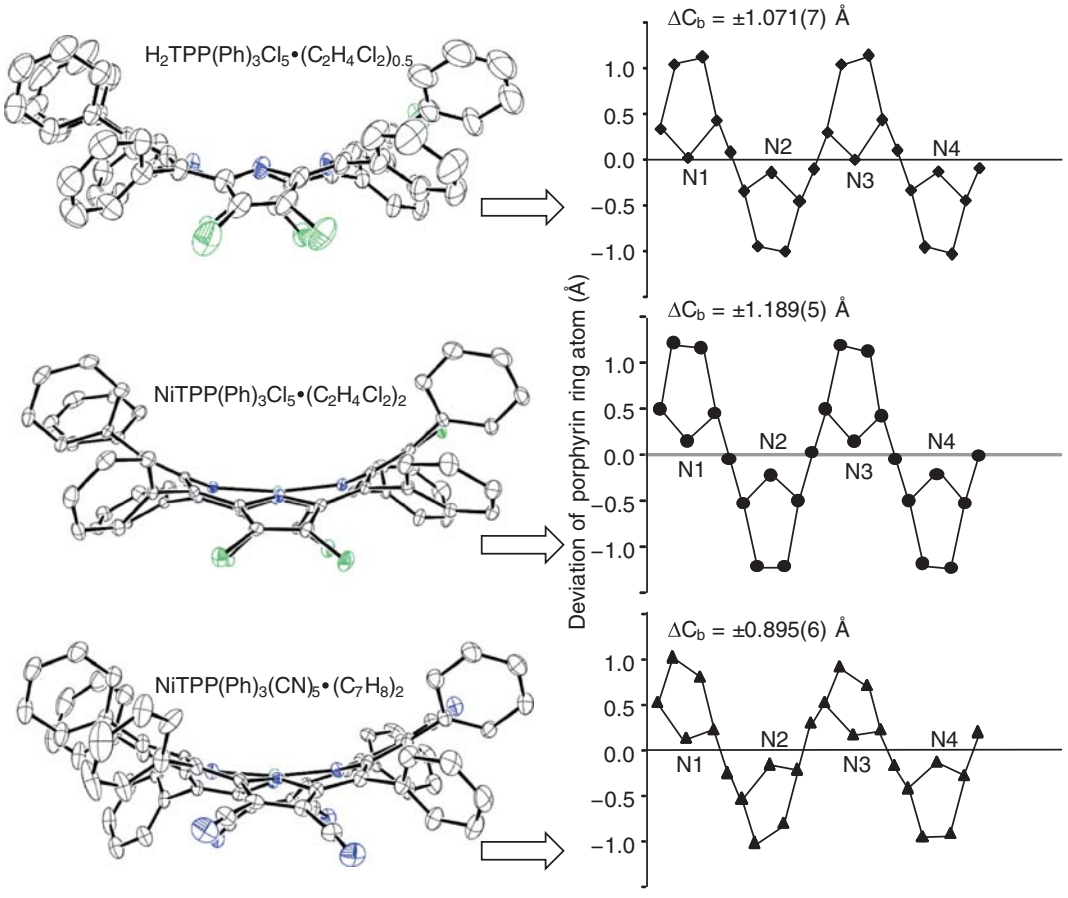

Figure 3. ORTEP diagrams shown on the left side are for structures (**1-3**) and on the right side the corresponding linear displacement of the 24-atom core is shown.

Table 3. Normal-coordinate structural decomposition analysis of structures **1-3**.

	Out-of plane-displacement in Å									
	D_{oop}	B_{2u}, *sad*	B_{1u}, *ruf*	A_{2u}, *dom*	$E_g(x)$, *wav(x)*	$E_g(y)$, *wav(y)*	A_{1u}, *prop*	*sum*	B_{2u}/*sum*, %	B_{1u}/*sum*, %	A_{2u}/*sum*, %
1	3.1287	3.1105	−0.2740	−0.1930	−0.0046	−0.0337	0.0137	3.629	85.7	7.5	5.3
2	3.6513	−3.6494	0.0736	0.0270	0.0405	−0.0152	−0.0730	3.879	94.1	1.9	0.7
3	2.8296	−2.7484	0.6411	−0.0699	−0.1745	−0.0194	−0.0768	3.730	73.7	17.2	1.9
	In-plane-displacement in Å										
	D_{ip}	B_{2g}, *m-str*	B_{1g}, *N-str*	$E_u(x)$, *Trn*	$E_u(y)$, *trn*	A_{1g}, *bre*	A_{2g}, *rot*	*sum*	B_{2g}/*sum*, %	B_{1g}/*sum*, %	A_{1g}/*sum*, %
1	0.5473	−0.0929	−0.2120	−0.0135	0.0066	−0.4955	−0.0144	0.835	11.1	25.4	59.3
2	1.0147	0.0141	−0.0537	0.0293	−0.0093	−1.0126	−0.0120	1.131	1.3	4.7	89.5
3	0.6632	−0.0121	−0.0057	−0.0079	−0.0157	−0.6628	−0.0083	0.713	1.7	0.8	92.9

intermolecular interactions.[56] The nonplanar distortion of the macrocycle in the structures **1-3** arise from steric crowding of the peripheral substituents and/or Ni(II) ion and weak intermolecular interactions. As reported previously, β-octasubstituted MTPPs (M = 2H or Ni(II)) showed increase in nonplanarity of the macrocycle.[27]

To examine the unsymmetrical mixed β-octasubstitution on the macrocyclic distortion modes, the crystal structures were analyzed by normal-coordinate structural decomposition analysis.[57] The in-plane (D_{ip}) and out-of-plane (D_{oop}) displacement values of the macrocycle based on the minimum basis set is listed in Table 3. The *sum* is calculated from the addition of absolute values of the individual displacements. The structures of **1-3** shows prominently *saddle* (73–95%) combined with small *ruffling* (2–18%) and *domed* (1–6%) deformations. Similar behavior was reported for the $H_2TPP(Ph)_4Cl_4$ (D_{oop} = 3.3055 Å) with mainly *saddle* distortion of the macrocycle.[42] The magnitude of the D_{oop} is similar to the reported β-octasubstituted MTPPs.[27] The trend in both D_{oop} and D_{ip} values varies in the order **1** < **3** < **2**. In the case of the in-plane-displacements of these structures, A_{1g} (59–93%) contributes mainly with varying degree of B_{1g} (1–26%)

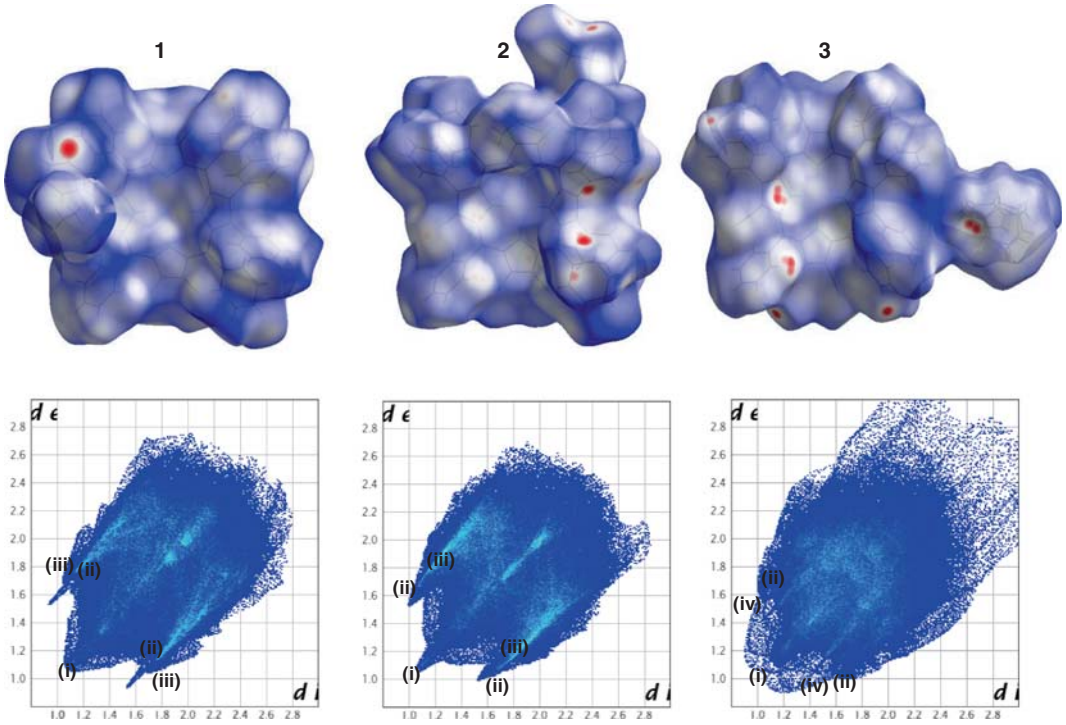

Figure 4. 3-D fingerprint for structures **1-3** are shown on top and below diagrams represent the 2-D fingerprint regions of the corresponding structures for major intermolecular contacts: (i) H. . .H; (ii) C. . .H; (iii) H. . .Cl and (iv) N. . .H.

Table 4. Summary of Hirshfeld surface analysis of solvated unsymmetrically mixed substituted porphyrin structures (**1-3**).

	$H_2TPP(Ph)_3(Cl)_5$, %	$NiTPP(Ph)_3(Cl)_5$, %	$NiTPP(Ph)_3(CN)_5$, %
H...H	48.3	43.2	53.6
C...H	16.8	17.4	18.9
H...Cl	26.4	30.0	–
N...H	3.1	2.5	19.5
C...Cl	2.9	2.4	–
C...C	0.5	0.7	3.2
N...C	1.0	0.8	2.4
Cl...Cl	0.4	1.0	–
N...Cl	0.6	0.6	–
Ni...C	–	0.1	0.3
Ni...H	–	1.2	0.8
Ni...N	–	–	0.1
N...N	–	–	1.0

and B_{2g} (1–12%) deformations. The enhanced deformation of the macrocycle in **2** relative to **3** suggests the extent of steric crowding around the periphery of the porphyrin ring.

The 3-D Hirshfeld surfaces of solvated structures **1**-**3** are shown in Figure 4 along with their 2-D fingerprint regions. The dark red spots on the 3-D surface shows the close contact regions mainly responsible for intermolecular hydogen-bonds. The summary of the contributions from various intermolecular interactions of Hirshfeld surface analysis for all the structures are given in Table 4. It can be seen from the 2-D fingerprint plots, that the middle region shows the most significant contribution for H...H interactions (43–54%) to the total Hirshfeld surface in both the structures and this contribution in structures **1** and **2** amounts to 49% and 43% respectively. Structures **1** and **2** feature similar intermolecular C...H contact contribution and it is slightly lower than that observed in **3**. The N...H contribution is significant owing to the peripheral pyrrole CN group interacting with the adjacent porphyrins in **3** and it is absent in structures **1** and **2**. The intermolecular interactions arising from C...C interactions is least in structures **1** and **2** and it is about 3% in structure **3**. The presence of chlorinated solvent and the chloro substituted porphyrin structures **1** and **2** revealed considerable H...Cl contribution (25–30%) with very small contribution from C...Cl intermolecular contacts. Other intermolecular contact contributions were negligibly small and they are also listed in Table 4.

4. Conclusions

Few structures of unsymmetrically β-functionalized porphyrins, $MTPP(Ph)_3X_5$ (M = 2H and Ni(II)) (**1** and **2**) and $NiTPP(Ph)_3(CN)_5$ (**3**) were determined by single crystal XRD analysis. These structures (**1-3**) exhibited nonplanar distortion of the macrocycle which is evident from the average displacement of the β-pyrrole carbon and it varies in the range $\Delta C_b = \pm$ (0.895(6) Å − 1.189(5) Å). The NSD analysis of the structures revealed mainly *saddle* distortion of the macrocycle combined with varying degree of *ruffled* and *domed* deformation. Interestingly, Hirshfeld surface analysis of structures showed solvate dependent intermolecular contact contributions. The nonplanar distortions in **2** and **3** is largely influenced by steric crowding of the peripheral substituents and the core Ni(II) ion than the intermolecular interactions. The sterically unhindered *meso*-tetrakis(2′, 6′/3′, 5′ -diflurophenyl)porphyrins and their Zn(II) and Cu(II) complexes exhibited significant changes in their conformation of the macrocycle upon switching the position of the fluoro groups.[58]

Acknowledgement

This work was supported financially from the grant-in-aid of the Department of Science and Technology (DST, Govt. of India) to PB. We thank Mr. V. Ramkumar for single crystal XRD data collection and department of Chemistry, IIT Madras for the XRD facility.

References

1. Kadish K M, Smith K M and Guilard R (Eds.) 2000–2013 In *Handbook of Porphyrin Science* Vol. 1–25 (London: World Scientific)
2. Senge M O 2005 *Acc. Chem. Res.* **38** 733
3. Lindsey J S 2010 *Acc. Chem. Res.* **43** 300 and references therein
4. Kosal M E, Chou J H, Wilson S R and Suslick K S 2002 *Nature Mater.* **1** 118

5. Suslick K S, Bhyrappa P, Chou J H, Kosal M E, Nakagaki S, Smithenry D W and Wilson S R 2005 *Acc. Chem. Res.* **38** 283
6. Dolphin D, Traylor T G and Xie L Y 1997 *Acc. Chem. Res.* **30** 251 and references therein
7. Ellis P E Jr and Lyons J E 1990 *Coord. Chem. Rev.* **105** 181
8. Hoffmann P Labat G, Robert A and Meunier B 1990 *Tetrahedron Lett.* **31** 1991
9. Lyons J E and Ellis P E 1991 *Catal. Lett.* **8** 45
10. Sheldon R A 1994 In *Metalloporphyrins in Catalytic Oxidations* (New York: Marcel Dekker)
11. Grinstaff M W, Hill M G, Labinger L A and Gray H B 1994 *Science* **264** 1311
12. Meunier B 1992 *Chem. Rev.* **92** 1411
13. Buehlmann P, Pretsch E and Bakker E 1998 *Chem. Rev.* **98** 1593
14. Kang Y, Kampf J W and Meyerhoff M E 2007 *Anal. Chim. Acta* **598** 295
15. Tu W, Lei J, Jian G, Hu Z and Ju H 2010 *Chem. Eur. J.* **16** 4120
16. Filippini D, Alimelli A, Natale C D, Paolesse R, D'Amico and Lundstrom I 2006 *Angew. Chem., Int. Ed.* **45** 3800
17. Badr I H A and Meyerhoff M E 2005 *J. Am. Chem. Soc.* **127** 5318
18. Rakow R A and Suslick K S 2000 *Nature* **406** 710
19. Rakow R A, Sen A, Janzen M A, Ponder J B and Suslick K S 2005 *Angew. Chem. Int. Ed.* **44** 4528
20. Senge M O, Fazekas M, Notaras E G A, Blau W J, Zawadzka M, Locos O B and Ni Mhuircheartaigh E M 2007 *Adv. Mater.* **19** 2737
21. Kalnoor B S, Bisht P B, Jena K C, Velkannan V and Bhyrappa P 2013 *J. Phys. Chem. A* **117** 8216
22. Urbani M, Grätzel M, Nazeeruddin M K and Torres T 2014 *Chem. Rev.* **114** 12330
23. Li L L and Diau E W G 2013 *Chem. Soc. Rev.* **42** 291
24. Hagfeldt A, Boschloo G, Sun L, Kloo L and Patterson H 2010 *Chem. Rev.* **110** 6595
25. Scheidt W R 2000 In *The Porphyrin Handbook* K M Kadish, K M Smith and R Guilard R (Eds.) Vol. 3 (San Diego: Academic Press) p. 49
26. Panda P K and Krishnan V 2005 *J. Chem. Sci.* **115** 73
27. Senge M O 2000 In *The Porphyrin Handbook* K M Kadish, K M Smith and R Guilard R (Eds.) Vol. 1 (San Diego: Academic Press) p. 239
28. Shelnutt J A, Song X Z, Ma J G, Jia S L, Jentzen W and Medforth C J 1998 *Chem. Soc. Rev.* **27** 31 and references therein
29. Renner M W, Furenlid L R, Barkigia K M, Forman A, Shim H K, Smith K M and Fajer J 1991 *J. Am. Chem. Soc.* **113** 6891
30. Shelnutt J A 2000 In *The Porphyrin Handbook* K M Kadish, K M Smith and R Guilard R (Eds.) Vol. 7 (San Diego: Academic Press) p. 167
31. Renner M W, Barkigia K M, Zhang Y, Medforth C J, Smith K M and Fajer J 1994 *J. Am. Chem. Soc.* **116** 8582
32. Sparks L D, Medforth C J, Park M S, Chamberlain J R, Ondrias M R, Senge M O, Smith K M and Shelnutt L A 1993 *J. Am. Chem. Soc.* **115** 581
33. Barkigia K M, Renner M W, Furenlid L R, Medforth C J, Smith K M and Fajer J 1993 *J. Am. Chem. Soc.* **115** 3627
34. Medforth C J, Senge M O, Smith K M, Sparks L D and Shelnutt J A 1992 *J. Am. Chem. Soc.* **114** 9859
35. Regev A, Galili T, Medforth C J, Smith K M, Barkigia K M, Fajer J and Levanon H 1994 *J. Phys. Chem.* **98** 2520
36. Senge M O and Kalisch W W 1997 *Inorg. Chem.* **36** 6103
37. Barkigia K M, Berber M D, Fajer J, Medforth C J, Renner M W and Smith K M 1990 *J. Am. Chem. Soc.* **112** 8851
38. Senge M O 2000 In *The Porphyrin Handbook* K M Kadish, K M Smith and R Guilard R (Eds.) Vol. 10 (San Diego: Academic Press)
39. Byrn M P, Curtis C J, Hsiou Y, Khan S I, Sawin P A, Tendick S A, Terzis A and Strouse C E 1993 *J. Am. Chem. Soc.* **115** 9480
40. Krupitsky H, Zafra S, Goldberg I and Strouse C E 1994 *J. Inclu. Phen. Mol. Recogn.* **18** 177
41. Senge M O, Gerstung V, Senge K R, Runge S and Lehmann I 1998 *J. Chem. Soc., Dalton Trans.* 4187
42. Bhyrappa P, Arunkumar C and Varghese B 2009 *Inorg. Chem.* **48** 3954
43. Bhyrappa P and Velkannan V 2010 *Tetrahedron Lett.* **51** 40
44. Velkannan V and Bhyrappa P 2015 *Polyhedron* **87** 170
45. Sheldrick G M, SHELXL97, 1997 *Program for the Refinement of Crystal Structures*; University of Göettingen: Göettingen, Germany
46. Altomare A G, Cascarano G, Giacovazzo C and Gualardi A 1993 *J. Appl. Crystallogr.* **26** 343
47. Spek A L 2003 *J. Appl. Crystallogr.* **36** 7
48. Bruno I J, Cole J C, Edgington P R, Kessler M, Macrae C F, McCabe P, Pearson J and Taylor J 2002 *Acta Cryst.* **B58** 389
49. Hirshfeld F L 1997 *Theor. Chim. Acta* **44** 129
50. Wolff S K, Grimwood D J, Mcinnon J J, Turner M J, Jayatilaka D and Spackman M A 2012 *Crystal Explorer 3.1* University of Western Australia
51. McKinnon J J, Spackman M A and Mitchell A S 2004 *Acta Crystallogr. Sect.* **B60** 627
52. Parkin A, Barr G, Dong W, Gilmore C J, Jayatilaka D, McKinnon J J, Spackman M A and Wilson C C 2007 *Cryst. Eng. Commun.* **9** 648
53. Spackman M A and McKinnon J J 2002 *Cryst. Eng. Commun.* **4** 378
54. Bhyrappa P, Senkar M and Varghese B 2006 *Inorg. Chem.* **45** 4136
55. Duval H, Balach V, Fischer J and Weiss R 1999 *Inorg. Chem.* **38** 5495
56. Desiraju G R and Steiner T 1999 In *The weak hydrogen-bonding in structural chemistry and Biology. IUCr monographs on Crystallography* (UK: Oxford University Press) p. 215
57. Jentzen A, Ma J M and Shelnutt J A 1998 *Biophys. J.* **74** 753
58. Bhyrappa P and Karunanithi K 2016 *J. Chem. Sci.* **128** 501